
Adaptive Aggregation for Safety-Critical Control

Huiliang Zhang, Di Wu and Benoit Boulet
Department of Electrical & Computer Engineering
McGill University
Montreal, QC H3A 0E9
huiliang.zhang2@mail.mcgill.ca

Abstract

Safety has been recognized as the central obstacle to preventing the use of reinforcement learning (RL) for real-world applications. Different methods have been developed to deal with safety concerns in RL. However, learning reliable RL-based solutions usually require a large number of interactions with the environment. Likewise, how to improve the learning efficiency, specifically, how to utilize transfer learning for safe reinforcement learning, has not been well studied. In this work, we propose an adaptive aggregation framework for safety-critical control. Our method comprises two key techniques: 1) we learn to transfer the safety knowledge by aggregating the multiple source tasks and a target task through the attention network; 2) we separate the goal of improving task performance and reducing constraint violations by utilizing a safeguard. Experiment results demonstrate that our algorithm can achieve fewer safety violations while showing better data efficiency compared with several baselines.

1 Introduction

Reinforcement learning (RL) is a key technique to build autonomous agents which can learn and adapt to the changes of environments. Recent advances in RL have led to rapid progress in domains such as Atari Mnih et al. [2015], Go Silver et al. [2017], manipulation Nagabandi et al. [2020], Sun et al. [2022], locomotion tasks Haarnoja et al. [2018], Li et al. [2021], and business Zhang et al. [2021], Ma et al. [2021]. However, deploying RL algorithms to real-world applications faces a hurdle with safety concerns. When venturing into new regions of the state space during the unconstrained exploration, the agent may cause unaccepted failures, such as unfavourable impacts to people, property and the agent itself Garcia and Fernández [2015], Chen et al. [2021], Thomas et al. [2021], Saboo et al. [2021]. Moreover, the safety constraints may also limit the agents' ability to explore the entire state and action space to maximize the expected total reward Thananjeyan et al. [2021]. Thus, achieving adaptability and maintaining good performance with constraints satisfaction is of importance for the widespread use of RL in the real world.

Most RL research endows agents with the ability to satisfy safety constraints from the line of control theory-based method or the constrained policy optimization formulation Chow et al. [2018], Thananjeyan et al. [2021]. Remarkably, those safe RL algorithms succeeded with surprisingly little access to prior knowledge about the experienced tasks. Though the ability to learn with minimal prior knowledge is desirable, it can lead to computationally intensive learning and limited exploration. Moreover, the control theory-based method learns a conservative safe region with the accurate dynamic model, which can remain no safety violations Chow et al. [2018], Lütjens et al. [2019], Cheng et al. [2019], Brown et al. [2020], Thomas et al. [2021], Paternain et al. [2022]. The constrained policy optimization uses an intervention mechanism to evaluate the safety or by adding the penalty in reward functions to suppress the unsafe policy Alshiekh et al. [2018], Thananjeyan et al. [2021], Cowen-Rivers et al. [2022]. Those two methods maintain good safety performance after the policy converged but may fail to work well in a new safety-critical settings Zhang et al. [2020], Laroche et al. [2019], Chen et al. [2021], harsh satija et al. [2021].

Transferring safety knowledge gained from tasks solved earlier to solve a new target safety-critical task can help, either in terms of speeding up the learning process or in terms of achieving a better performance Laroche et al. [2019], Zhang et al. [2020], Turchetta et al. [2020], Chen et al. [2021]. The existing transfer RL approaches such as Rajendran et al. [2015] (A2T) and Barekatin et al. [2021] (A2S) were evaluated on the 36th Conference on Neural Information Processing Systems (NeurIPS 2022).

[2019] (MULTIPOLAR) omit the safety requirements which could lead to costly failure. A2T also fails to deal with partially useful policies and MULTIPOLAR can't attend to the changes of input states directly. Plus, safe policy reuse methods assume an optimal safe policy and focus on selecting a suitable source policy for explorations. They are also unable to handle cases when the source policy is only partially useful for learning the target task Zhang et al. [2020], Turchetta et al. [2020] (CARL and CISR). Although some transfer approaches have utilized multiple source policies during the target task learning, they have strong assumptions on the guaranteed relatedness between source and target tasks Turchetta et al. [2020], Chen et al. [2021]. Moreover, we cannot rely on a history of their individual experiences, as they may be unavailable due to a lack of communication between factories or prohibitively large dataset sizes Chen et al. [2021], Laroche et al. [2019], Turchetta et al. [2020], Thananjeyan et al. [2021], and cannot assure the non-safety violations during the training and deployment.

To tackle the aforementioned challenges, we propose to use transfer learning to improve the learning efficiency in safe RL. Specifically, inspired by Rajendran et al. [2015], Barekatin et al. [2019], we propose an adaptive aggregation architecture in safety-critical (AASC) control which reuses knowledge from multiple sources solutions. Our key idea is twofold; 1) The safety knowledge transfer by aggregating multiple source tasks and a target task through attention and auxiliary network. By learning aggregation parameters to maximize the expected return at a target environment instance, we can adapt quickly thus improving the learning efficiency in unseen target tasks without knowing source environmental dynamics or source policy performances. Plus, the agent can decide which source solution to attend or suppress to, or to choose the solution from the auxiliary when the source tasks are irrelevant to solving the target task. 2) We separate the goals of improving task performance and constraint satisfaction by utilizing a safeguard to improve safety performance. This separation allows the learned task policy to purely focus on collecting the most informative experiences and can maintain safety during training and deployment. We also empirically validate AASC by comparing its performance with several standard transfer RL and safe RL algorithms in simulated control tasks. Our experimental results demonstrate the significant improvement in learning efficiency and safety performance with the proposed approach. We also conducted a detailed analysis of factors that affect the performance of AASC, and demonstrate that the AASC is an effective and generic framework for safe RL.

2 Preliminaries

2.1 Safe reinforcement learning

We consider safe RL in a γ -discounted infinite horizon MDP M . An MDP can be expressed as a tuple $M = \langle S, A, P, R, \gamma \rangle$, where S, A, P and R are the sets of states s_t , actions a_t , state transition probabilities p and rewards r ; $\gamma \in [0, 1]$ is a discount factor accounting for future rewards. A policy π induces a trajectory distribution. For a state distribution $d \in \Delta(S)$ and function $f : s \rightarrow \mathbb{R}$, we define $f(d) = \mathbb{E}_{s \sim d}[f(s)]$. The initial state distribution of π is d_0^π and the average state distribution induced by π is $d^\pi = (1 - \gamma) \sum_{t=0}^{\infty} \gamma^t d_t^\pi(s)$. The state-action value function of π is defined as $Q^\pi(s, a) = \mathbb{E}_{\xi \sim \rho^\pi | s_0=s, a_0=a} [\sum_{t=0}^{\infty} \gamma^t r(s_t, a_t)]$ and its state value function as $V^\pi(s) = Q^\pi(s, \pi)$. The optimal stationary policy of M is π^* and its respective value function are Q^* and V^* .

The definition of safety is that the probability of the agent entering an unsafe subset of state $S_{unsafe} \subset S$ is low, which is consistent with Thomas et al. [2021], Thananjeyan et al. [2021], Wagener et al. [2021]. We assume that we know the unsafe subset S_{unsafe} and the safe subset $S_{safe} = S \setminus S_{unsafe}$. However, we make no assumption on the knowledge of reward r and dynamics P , except that the reward r is zero on S_{unsafe} and that S_{unsafe} is absorbing: once the agent enters S_{unsafe} in a rollout, it cannot travel back to S_{safe} and stays in S_{unsafe} for the rest of the rollout. Our goal is to find a policy π that is safe and has a high return in M , and to do so via a safe data collection process, which is shown as follows:

$$\pi^* = \underset{\pi}{\operatorname{argmax}} \{V^\pi(d_0) : (1 - \gamma) \sum_{h=0}^{\infty} \gamma^h \operatorname{Prob}(\xi_h \subset S_{safe} | \pi) \geq 1 - \delta\} \quad (1)$$

where $\xi_h = (s_0, a_0, s_1, a_1, \dots, s_{h-1}, a_{h-1})$ denotes an h -step trajectory segment and $\delta \in [0, 1]$ is the tolerated failure probability. $\operatorname{Prob}(\xi_h \subset S_{safe} | \pi)$ denotes the probability of ξ_h being safe (i.e., not entering absorbing state from time step 0 to $h - 1$) under the trajectory distribution ρ^π of π on M . An initial state drawn from d_0 is assumed to safe with probability 1. The constraint shown

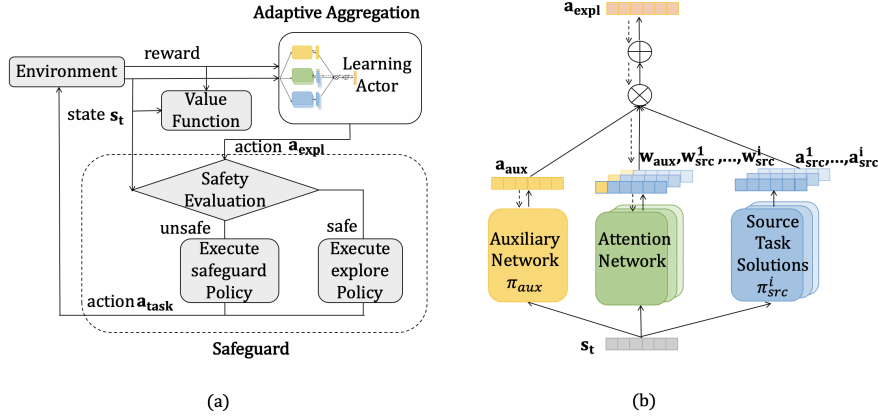


Figure 1: (a) Overview of AASC architecture. The adaptive aggregation module learns the exploratory action a_{expl} and the safeguard module ensures the safety during the learning process and output task safe action a_{task} . (b) Adaptive aggregation of safe policies. We formulate the aggregated policy π_{expl} with the sum of 1) the adaptive aggregation of actions from source policies π_{src} and 2) the auxiliary network π_{aux} for predicting residuals a_{aux} . The dotted arrows represent the path of back propagation.

in equation (1) is known as a chance constraint. The definition here accords to an exponentially weighted average (based on the discount factor γ) of trajectory safety probabilities of different horizons. Then the problem in equation (1) can be formulated as a constrained MDP (CMDP) problem with extra constraint cost function $C : S \times A \rightarrow \{0, 1\}$ with associated discount factor γ_{risk} which indicates whether state action is constraint violating. This yields the following new CMDP: $\bar{M} = \langle S, A, P, R, \gamma, C, \gamma_{risk} \rangle$. And \bar{M} consists with M and a cost-based MDP ($\bar{M} = \langle S, A, P, C, \gamma_{risk} \rangle$). The chance-constrained policy optimization in (1) corresponds to the CMDP formulation from Efroni et al. [2020] can be written as:

$$\pi^* = \operatorname{argmax}_{\pi} \{V^{\pi}(d_0) : \bar{V}^{\pi}(d_0) \leq \delta\} \quad (2)$$

where $\bar{V}^{\pi}(s) = \bar{Q}^{\pi}(s, \pi)$ and $\bar{Q}^{\pi}(s, a) = \mathbb{E}_{\xi \sim \rho^{\pi} | s_0=s, a_0=a} [\sum_{t=0}^{\infty} \gamma_{risk}^t c(s_t, a_t)]$. Equation (2) aims to find a policy that has a high cumulative reward $V^{\pi}(d_0)$ with cumulative cost $\bar{V}^{\pi}(d_0)$ below the allowed failure probability δ . We assume that episodes terminate on violations, equivalent to transitioning to a constraint-satisfying absorbing state with zero reward.

2.2 Transfer reinforcement learning

Transfer RL aims at improving the learning efficiency of an agent by exploiting knowledge from other agents trained on source tasks Barekatin et al. [2019]. Source tasks refer to tasks that we have already learnt to perform and target task refers to the task that we are interested in learning now. Here the source tasks should be in the same domain as the target task, having the same state and action spaces. Let there be I source tasks which correspond to I instances of the same environment which differ only in their state transition dynamics. Namely, we model each environment instance by an indexed MDP: $M_i = \langle S, A, P_i, R, \gamma \rangle$ where no two-state transition distributions $P_i, P_j, i \neq j$ are identical. We assume that each P_i is unknown when training a target policy, i.e., agents cannot access the exact form of P_i nor a collection of states sampled from P_i . For each of the I environment instances, we are given a source policy solution $\pi_{src}^i : S \rightarrow \Delta(A)$ that only maps states to actions. These solutions could be for example policies or state-action values.

3 Adaptive aggregation in safety-critical (AASC) control

In this section, we elaborate on the framework of AASC in safe RL settings, including the adaptive aggregation of safety policies and the safeguard evaluation parts. In safety-critical settings, humans tend to query the knowledge learned before solving similar problems and get a potential solution. Then they will evaluate the safety of the potential solution and decided whether to execute it in real life. The solution with safety constraints satisfaction could be found quickly in this manner. Thus,

the AASC consists of two parts: **the adaptive aggregation of safety policies** and **the safeguard evaluation**, as shown in figure 1 (a). The former helps us to efficiently learn the safe policy of a target agent given a collection of source policies, which inspired by Rajendran et al. [2015], Berekatain et al. [2019], the latter ensures the safety constraints and maximizes the final performance in the safety-critical settings, inspired by Bharadhwaj et al. [2020], Wagener et al. [2021].

The proposed method optimizes policies iteratively as outlined in Algorithm 1. As input, it takes an AASC algorithm \mathcal{F} with a safe policy aggregation and safeguard module and multi-source tasks solutions π_{src} . The RL algorithm \mathcal{F} finds a nearly optimal policy for the MDP \widetilde{M} constructed by the safeguard together with M , which is an approximate solution of equation (2). During training, the agent can interact with the unknown MDP M to collect data under a training budget, such as the maximum number of environment interactions or allowed unsafe trajectories the agent can generate. In every iteration, the proposed method first queries the safe policy aggregation of \mathcal{F} to have a potential exploratory action a_{expl} to execute in \widetilde{M} . Then it uses a safeguard policy to modify exploratory action into task safe action a_{task} . The safeguard module is a shielded policy such that the agent runs backup policy $\mu : S \rightarrow \Delta(A)$ instead of π_{expl} when π_{expl} proposed unsafe actions. Then running a_{task} in the M can be safe with high probability. Next, it collects data by running a_{task} in M and collects data into \mathcal{D}_{task} then transforms it into data $\mathcal{D}_{Safeguard}$. The transition stores in \mathcal{D}_{task} is $\langle s_t, a_{task}, s_{t+1}, r_t \rangle$ and $\langle s_t, a_{expl}, s_{t+1}, r_t, c_t \rangle$ in $\mathcal{D}_{Safeguard}$. It then feeds \mathcal{D}_{task} to the \mathcal{F} for policy optimization and uses $\mathcal{D}_{Safeguard}$ to refine the shield policy. The process above is repeated until the training budget is used up. When this happens, it terminates and returns the best policy $\hat{\pi}^*$ from algorithm \mathcal{F} can produce.

3.1 Adaptive aggregation of safe policies

The goal of this adaptive aggregation of safe policies is to train a new target agent’s policy π_{task} in a sample efficient fashion. The target agent interacts with the target environment instance which is not identical to the source due to their distinct dynamics. For each of the I source tasks, we are given the source policy $\pi_{src}^i : S \rightarrow A$ that only maps states to actions. Each source policy π_{src}^i can be either parameterized (e.g., learned by interacting with its environment instance M_i) or non-parameterized (e.g., heuristically designed by humans). Either way, we assume that no prior knowledge about the source policies π_{src}^i is available for a target agent, such as their representations of original performances, except that they were acquired from a source environment instance with an unknown dynamics. As shown in figure 1 (b), with the adaptive aggregation of safety policies, a target policy is formulated with the adaptive aggregation of actions from the set of source policies, and the auxiliary network mimicking the selected policies and predicting residuals around the aggregated actions. Let $a_{src}^1, a_{src}^2, \dots, a_{src}^I$ be the solutions of these source tasks $1, \dots, I$ respectively. a_{aux} is the solution of an auxiliary network that starts learning from scratch while acting on the target task. Let a_{expl} be the solution that we learn in the target task. The action space $a_t^i \in \mathbb{R}^D$ is a D -dimensional real-valued vector representing D actions performed jointly in each timestep. For the collection of source policies, we derive the matrix of their actions:

$$A_t = [(a_{src}^1)^T, \dots, (a_{src}^I)^T, (a_{aux})^T] \in \mathbb{R}^{(I+1) \times D} \quad (3)$$

Algorithm 1 Adaptive Aggregation in Safety-Critical (AASC) Control

Input: AASC RL algorithm \mathcal{F} , $\mathcal{D}_{task} \leftarrow \emptyset$, $\mathcal{D}_{Safeguard} \leftarrow \emptyset$, multi-source tasks solutions π_{src} .

Output: Optimized safe policy $\hat{\pi}^*$

- 1: \mathcal{F} .Initialize()
 - 2: $s \leftarrow \text{env.reset}()$
 - 3: **while** training budget available **do**
 - 4: $a_{expl} \leftarrow \mathcal{F}$.SafePolicyAggregation(s, π_{src})
 - 5: $a_{task} \leftarrow \mathcal{F}$.Safeguard(s, a_{expl})
 - 6: Execute a_{task} and collect data to \mathcal{D}_{task} and $\mathcal{D}_{Safeguard}$, $s = s'$
 - 7: $\hat{\pi} \leftarrow \mathcal{F}$.OptimizePolicy(\mathcal{D}_{task})
 - 8: \mathcal{F} .UpdateSafeguardRule($\mathcal{D}_{Safeguard}$)
 - 9: **end while**
 - 10: $\hat{\pi}^* \leftarrow \mathcal{F}$.GetOptimizePolicy()
-

Algorithm 2 Adaptive Aggregation of Safety Policies

Input: State s , multi-source tasks solutions π_{src}

Output: Adaptive aggregation action a_{expl}

- 1: **for** $i \in \{1, \dots, I\}$ **do**
 - 2: Calculate $a_{src}^i \sim \pi_{src}^i(\cdot|s)$
 - 3: Calculate $a_{aux} \sim \pi_{aux}(\cdot|s)$
 - 4: Calculate $w_{aux}, w_{src}^1, w_{src}^2, \dots, w_{src}^I$
 - 5: Calculate a_{expl} according to equation (4).
-

The key idea of the aggregation module is to aggregate A_t adaptively in an RL loop, i.e., to maximize the expected return $V^\pi(d_0)$. The adaptive aggregation only contains the source policies action that could introduce a strong inductive bias in the training of a target policy. So we learn an auxiliary policy network as $\pi_{aux} : S \rightarrow \Delta(A)$ jointly with the source task policy, to predict residuals around the aggregated source task actions. π_{aux} is used to improve the target policy training in two ways. 1) If the aggregated actions from π_{src} are already useful in the target environment instance, a_{aux} will correct them for a higher expected return. 2) Otherwise, π_{aux} learns the target task while leveraging π_{aux} as a prior to have a guided exploration process. Any network could be used for a_{aux} as long as it is parameterized and fully differentiable.

While the source task solutions $a_{src}^1, a_{src}^2, \dots, a_{src}^I$ remain fixed, the auxiliary network solutions are learnt and hence a_{aux} can change over time. There is an attention network to learn the weights $w_{aux}, w_{src}^1, w_{src}^2, \dots, w_{src}^I$ given the input state s_t . The weights determine the attention each actions gets, allowing the agent to selectively accept or reject the different actions, depending on the input states. The aggregation policy is formulated as:

$$a_{expl} = W_t \odot A_t \quad (4)$$

where $W_t = [w_{src}^1, w_{src}^2, \dots, w_{src}^I, w_{aux}] \in \mathbb{R}^{(I+1) \times D}$ is the weight matrix. \odot is the element-wise multiplication. W_t is neither normalized nor regularized and can scale each action of each policy independently. In this way, we can flexibly emphasize informative source actions while suppressing irrelevant ones. If the i source task solution's action is useful at state s , then the corresponding element in w_{src}^i is set to a high value by the attention network. Working at the granularity of states allows the attention network to attend to different source tasks, for different parts of the state space of the target task, thus giving it the ability to select informative actions. For parts of the state space in the target task, where the source task solutions are not relevant or even perform badly, the attention network learns to give high weight to the auxiliary network solution (which can be learnt and improved), thus avoiding bad source actions. The adaptive safe policy aggregation is shown in algorithm 3.

Depending on the feedback obtained from the environment upon following a_{expl} , the attention network's parameters are updated to improve performance. As mentioned earlier, the source task solutions, $a_{src}^1, a_{src}^2, \dots, a_{src}^I$ remain fixed. Updating these source task's parameters would cause a significant amount of unlearning in the source tasks solutions and result in a weaker transfer, which we observed empirically. Even though the agent follows a_{expl} , we update the parameters of the auxiliary network that produces a_{aux} , as if the action taken by the agent was based only on a_{aux} . Due to this special way of updating a_{aux} , a_{aux} also uses the valuable experience got by using a_{expl} which uses the solutions of the source tasks as well. This also means that, if there is a source task whose solution a_{src}^i is useful for the target task in some parts of its state space, then a_{aux} tries to replicate a_{src}^i in those parts of the state space. In practice, the source task solutions though useful might need to be modified to suit perfectly the target task. The auxiliary network takes care of these modifications required to make the useful source task solutions perfect for the target task. The special way of training the auxiliary network assists the architecture in achieving this faster.

3.2 Safeguard evaluation

The goal of safeguard evaluation is to evaluate the safety given the potential actions a_{expl} under the given states, and to guide the agent to safety when there are constraint violations likely. Most prior work in safe RL integrates constraint satisfaction into the task objective to jointly optimize the two and detect those regions. However, the inherent objective conflict exploration and constraints can lead to suboptimzilities in policy optimization. In the proposed safeguard, we consider an RL formulation subject to constraints on the probability of unsafe future behaviour and design the algorithm that

Algorithm 3 Safeguard Evaluation

Input: State s , adaptive aggregation action a_{expl}

Output: task safe action a_{task}

- 1: **if** $s, a_{expl} \in \mathcal{T}_{unsafe}^\pi$ **then**
 - 2: $a_{task} \sim \pi_{backup}(\cdot|s)$
 - 3: **else**
 - 4: $a_{task} = a_{expl}$
-

can balance the often conflicting objectives of task-directed exploration and safety, which is inspired by Thananjeyan et al. [2021], Wagener et al. [2021]. The agent evaluates the safety of a_{expl} in the safeguard module, and instead executes approximate resets to nearby safe states when constraint violation is probable.

To quantify the risk of entering an unsafe state, the safeguard rule is specified by a tuple $\mathcal{G} = \langle \bar{Q}, \mu, \eta \rangle$, where $\bar{Q} : S \times A \rightarrow [0, 1]$ is a state-action risk value estimator, η is a threshold and μ is a backup safeguard action from π_{backup} policy Thananjeyan et al. [2021]. π_{backup} is supposed to safeguard the exploration. As shown in algorithm (3), when sampling a_{task} from safeguard policy, it first queries if $(s, a_{expl}) \in \mathcal{T}_{unsafe}^\pi$ then it samples a_{task} according to π_{backup} . Otherwise executes $a_{task} = a_{expl}$. However, activating the backup policy too often is undesirable, as it only collects data from π_{backup} so there will be little exploration. Hence we define the unsafe set \mathcal{T}_{unsafe}^π in safeguard as:

$$\begin{aligned} \mathcal{T}_{unsafe}^\pi &= \{(s, a) \in S_{safe} \times A : \bar{A}(s, a) \geq \eta\} \\ \mathcal{T}_{safe}^\pi &= S \times A \setminus \mathcal{T}_{unsafe}^\pi \end{aligned} \quad (5)$$

and advantage cost function is:

$$\bar{A}(s, a) = \bar{Q}(s, a) - \bar{Q}(s, \mu) \quad (6)$$

The equation (5) and (6) mean that we have assumption: for all $(s, a) \in \mathcal{T}_{unsafe}^\pi$ that can be reached from d_0 with some policy, there exist some $a \in A$ such that $\bar{A}(s, a) = \bar{Q}(s, a) - \bar{Q}(s, \mu) \geq \eta$. In other words, for every state action we can reach from d_0 that will be overridden, there is an alternative action in the agent’s action space A that keeps the agent’s policy being safe. By running the safeguard evaluation constructed by the advantage function \bar{A} , our method controls the safety relative to the backup policy μ concerning d_0 . If the relative safety for each time step (i.e., advantage) is close to zero, then the relative safety overall is also close to zero (i.e. $\bar{V}^\pi(d_0) \leq \delta$). Note that the safeguard while satisfying $\bar{V}^\pi(d_0) \leq \delta$, can generally visit (with low probability) the states where $\bar{V}^\mu(s) > 0$ (e.g., = 1). At these places where μ is useless for safety, the safeguard rule naturally deactivates and lets the learner explore, which avoids the overly conservative safe region in Thananjeyan et al. [2021], Bharadhwaj et al. [2020]. When the agent takes some actions $(s, a) \in \mathcal{T}_{unsafe}^\pi$ in \tilde{M} , it goes to an absorbing state and receives a negative reward as shown in equation (7) and figure (2). Thus, the MDP \tilde{M} gives larger penalties for taking backup safe state-actions than for going into S_{unsafe} . This design ensures that any nearly-optimal policy of \tilde{M} will (when running in M) have a high reward

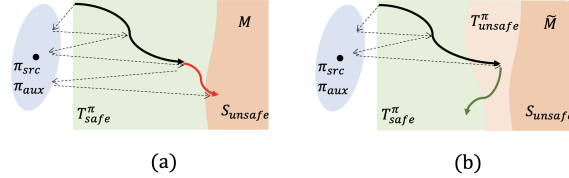


Figure 2: Safeguard Evaluation. (a) The agent in AASC starts in the safe states and follows the policy which is projected from the source and auxiliary policies. Without the safeguard evaluation, the agents may execute the disadvantaged action and have safety violations as red path. (b) Under the protection of safeguard, the backup policy will be activated and guide the agent to safety as green path.

and low probability of visiting safety violations state-actions.

$$\tilde{r}(s, a) = \begin{cases} b, & (s, a) \in \mathcal{T}_{unsafe}^\pi \\ 0, & s \text{ is an absorbing state} \\ r, & (\text{otherwise}). \end{cases} \quad (7)$$

where $b \leq 0$ is independent non-positive constant.

4 Experiments evaluation

4.1 Experiments setup

To showcase the effectiveness of the proposed method, we test its performance on two different simulated environments, i.e., Circle and Half-cheetah (figure 3). To ensure fair comparisons and reproducibility of experiments, we followed the guidelines introduced by François-Lavet et al. [2018] for conducting and evaluating all of our experiments.

Baseline methods: We implement AASC by using PPO (Schulman et al. [2017]) as the base RL model. To complete the experiments in a reasonable amount of time, we set the number of source policies to be $I = 4$ unless mentioned otherwise. The source policies are randomly sampled from the source policy candidates. See appendix A for all the implementation details. We also compared our AASC to the standard multi-layer perceptron (MLP) trained from scratch, which is typically used in RL literature François-Lavet et al. [2018]. As another baseline, we use **MULTIPOLAR** Barekatain et al. [2019] which selects source policies through an adjustable matrix. Also, we consider multi-source policy reuse framework **CARL** Zhang et al. [2020]. In all the experiments, source policies are the same for AASC, MULTIPOLAR and CARL to ensure an unbiased evaluation. The following CMDP-based approach which enforce constraints via the optimization objective **CPO** Achiam et al. [2017] is also considered. And the **Recovery RL** Thananjeyan et al. [2021] which uses ideas from offline RL to pretrain the recovery policy and designs a recovery rule directly based on Q-based functions is also compared.

Environment: Circle: The circle environment (figure 3 (a)) is the point environment from Achiam et al. [2017]. The agent is rewarded for running in a wide circle but is constrained to stay within a safe region smaller than the radius of the target circle while remaining in a circular path at high speed. The agent has mass m and can achieve maximum speed v_{max} . The safe set to staying within desired positional bounds x_{max} and y_{max} , as shown in the green space in the left of figure 3: $S_{safe} = \{s \in S : |x| \leq x_{max} \text{ and } |y| \leq y_{max}\}$ The backup policy μ applies a decelerating force (with component-wise magnitude up to a_{max}) until the agent has zero velocity. **Half-Cheetah:** The Half-Cheetah environment (figure 3 (b)) comes from OpenAI Gym and has a reward equal to the agent’s forward velocity. One of the agent’s links (green circle in the right of figure 3:) is constrained to lie in a given height range, outside of which the robot is deemed to have fallen over. In other words, if h is the height of the link of interest, h_{min} is the minimum height, and h_{max} is the maximum height, the safe set is defined as $S_{safe} = \{s \in S : h_{min} \leq h \leq h_{max}\}$. The agent gets a reward equal to its forward velocity, with one of its links constrained to remain in a given height range, outside of which the robot is deemed to be unsafe.

Evaluation metric: Following the guidelines of François-Lavet et al. [2018], to measure the sampling efficiency of training policies, i.e., how quickly the training progresses, we used the average episodic reward over training samples. Furthermore, we also report the cumulative constraint violations to

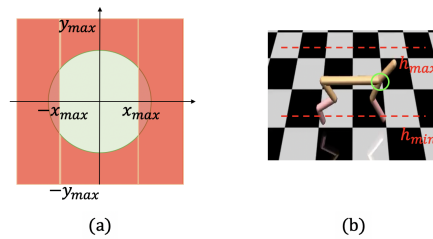


Figure 3: (a) The Circle environment. The agent can run in the green space. The green circle is the desired path, and the red lines are the constraints on the horizontal position. The vertical constraints are outside of the visualized environment. (b) The Half-cheetah environment. The green circle is centred on the link of interest, and the red dashed lines denote the allowed height range of the link.

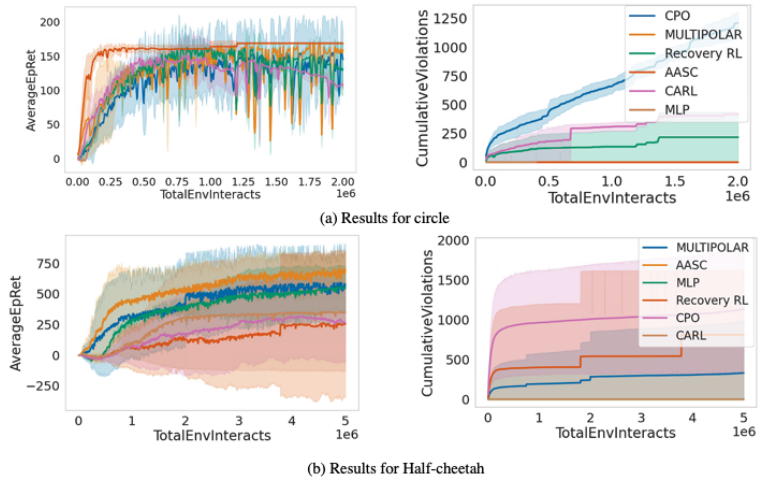


Figure 4: Results of MLP, MULTIPOLAR, CARL, CPO, Recovery RL and AASC over all the experiments for each environment. Overall AASC dramatically reduces the amount of training time and safety constraint violations while still having large returns at deployment. Plots in a row share the same legend. All error bars are ± 1 standard deviation over 5 random seeds. Any curve not plotted in the third column corresponds to zero safety violations.

show the safety performance of the proposed method. We tune all algorithms to maximize the total return to see the safety performance. Each run for simulation experiments is replicated across 5 random seeds and we report the mean and standard error.

4.2 Evaluation results

We study the learning and safety performance of the AASC and prior methods in all simulation domains in figure 4. Results suggest that AASC significantly improve the learning efficiency remain fewer safety violations than prior algorithms across two environments (Circle and Half-cheetah), which is of consistency with the motivation of our algorithm. The left column of figure 4 clearly shows that on average, AASC outperformed baseline policies in terms of sample efficiency and sometimes the final episodic reward. For example, the AASC converges faster at the early training stage than MLP and CPO in both environments, which indicates the effectiveness of leveraging multiple source policies in adaptive aggregation module. Compared with transferred RL methods such as CARL and MULTIPOLAR, AASC has always been on par or better performance on the sample efficiency. Because the aggregation module in AASC avoids the estimation of model error and leverages the change of the environment states as input, and can flexibly aggregate each action of each source policy.

The right column of figure 4 illustrates that the AASC prevents many safety violations. The safeguard in AASC is an unconstrained approach and allows for reliable convergence, as opposed to the baselines which rely on elaborate constrained approaches like CPO. AASC also incurs orders of magnitude fewer safety violations than Recovery RL and CARL, since the advantage-based safety evaluation is used and no model estimation error is accumulated, thus voiding the overly conservative safe region in exploration. More ablation studies could be found in appendix B, where we conduct a detailed analysis of factors that affect the performance of AASC, and demonstrate that the AASC is an effective and generic framework for safe RL.

5 Related work

5.1 Safe reinforcement learning

Many safe RL works on endowing RL agents with the ability to satisfy constraints from the line of control theory-based and the constrained policy optimization formulation approaches. A recent line of works on safe RL utilizes ideas from control theory and model-based approach Cheng et al. [2019], Zeng et al. [2021], Luo and Ma [2021], Chow et al. [2018], Thomas et al. [2021], Cowen-Rivers et al. [2022]. These works propose sufficient conditions involving certain Lyapunov functions or control barrier functions that can certify the safety of a subset of states or policies. Chow et al.

[2018] constructs sets of stabilizing actions using a Lyapunov function and projects the action to the set. Cheng et al. [2019] uses a barrier function to safeguard exploration and uses a reinforcement learning algorithm to learn a policy. Then Luo and Ma [2021] learns a barrier function to substitute the handcrafts one in Cheng et al. [2019]. From which the agent not only finds a high-return policy but also avoids undesirable states as much as possible, even during training. However, the works on Lyapunov functions require the discretizing of the state space and thus only work for low-dimensional space. And the barrier function-based method suffers from the sample efficiency and the bias of learned dynamics model problems Thomas et al. [2021], Cowen-Rivers et al. [2022].

Another line of works design the actor-critic based algorithms under the constrained policy optimization formulation. This line could also be divided into two groups: jointly optimizing the task performance and safety and restricting exploration with an auxiliary policy. Geibel and Wysotzki [2005] uses a Lagrangian method to solve CMDP, and the Lagrangian multiplier is controlled adaptively Tessler et al. [2018]. Paternain et al. [2022] uses the first-order primal-dual optimization to solve a stochastic nonconvex saddle-point problem in CMDP, but such approaches have no guarantees of policy safety during learning. Dalal et al. [2018] adds an additional layer, which corrects the output of the policy locally. However, these approaches make safe and optimal performance trade-offs. Then Bharadhwaj et al. [2020] learns a conservative safety critic who underestimates how safe the policy is, and uses the conservative safety critics for safe exploration and policy optimization. Thananjeyan et al. [2021] makes use of existing offline data and co-trains a conservative recovery policy based on the cost-based value function. In Wachi et al. [2021], the authors utilize the sensors data to make the features states available, and use linear function approximation to ensure the safety performance in the discrete control environment.

5.2 Transfer reinforcement learning

Transfer RL aims at improving the learning efficiency of an agent by exploiting knowledge from other source agents trained on relevant tasks. Song et al. [2016] transfers the action-value functions of the source tasks to the target task according to a task similarity metric to compute the task distance. However, they assume a well-estimated model which is not always available in practice. Later, Larocche and Barlier [2017] reuses the experience instances of a source task to estimate the reward function of the target task. Fernández and Veloso [2006] uses the policy reuse method as a probabilistic bias when learning the new, similar tasks. Rajendran et al. [2015] proposes the A2T (Attend, Adapt and Transfer) architecture to select and transfer from multiple source tasks by incorporating an attention network that learns the weights of several source policies for combination. Barekattain et al. [2019] uses an adjustable matrix, named MULTIPOLAR, to flexibly utilize the source policies, but omits the influence of the target environment on the selection of source solutions. Currently, there are only a few works considering leveraging learned policy Zhang et al. [2020], Chen et al. [2021] in safety-critical control. Zhang et al. [2020] employs model-based RL named CARL to train a probabilistic model to capture uncertainty about transition dynamics and catastrophic states across varied source environments. Chen et al. [2021] proposes the context-aware safe reinforcement learning method as a meta-learning framework to realize safe adaptation in non-stationary environments, which rely on a history of individual experiences.

6 Conclusion

In this work, we propose an adaptive aggregation framework for safety-critical control, which aims to improve sample efficiency and safety performance. We first learn to aggregate the safe actions provided by the source policies adaptively to maximize the target task performance. Meanwhile, we learn an auxiliary network that predicts residuals around the aggregated safe actions, which ensures the target policy’s expressiveness even when some of the source policies perform poorly. What’s more, we separate the constraints and explorations and use an advantaged safeguard evaluation to ensure safety during the learning process. Separating the task and safeguard policies makes it easier to balance task performance and safety, and allows using off-the-shelf RL algorithms for both. Empirically, our algorithm compares favourably to state-of-the-art safe RL methods, in terms of the trade-off between the learning and safety performance, and can achieve higher sample efficiency.

References

- Volodymyr Mnih, Koray Kavukcuoglu, David Silver, Andrei A Rusu, Joel Veness, Marc G Bellemare, Alex Graves, Martin Riedmiller, Andreas K Fidjeland, Georg Ostrovski, et al. Human-level control through deep reinforcement learning. *nature*, 518(7540):529–533, 2015.
- David Silver, Julian Schrittwieser, Karen Simonyan, Ioannis Antonoglou, Aja Huang, Arthur Guez, Thomas Hubert, Lucas Baker, Matthew Lai, Adrian Bolton, et al. Mastering the game of go without human knowledge. *nature*, 550(7676):354–359, 2017.
- Anusha Nagabandi, Kurt Konolige, Sergey Levine, and Vikash Kumar. Deep dynamics models for learning dexterous manipulation. In *Conference on Robot Learning*, pages 1101–1112. PMLR, 2020.
- Charles Sun, Jędrzej Orbik, Coline Manon Devin, Brian H Yang, Abhishek Gupta, Glen Berseth, and Sergey Levine. Fully autonomous real-world reinforcement learning with applications to mobile manipulation. In *Conference on Robot Learning*, pages 308–319. PMLR, 2022.
- Tuomas Haarnoja, Aurick Zhou, Kristian Hartikainen, George Tucker, Sehoon Ha, Jie Tan, Vikash Kumar, Henry Zhu, Abhishek Gupta, Pieter Abbeel, et al. Soft actor-critic algorithms and applications. *arXiv preprint arXiv:1812.05905*, 2018.
- Zhongyu Li, Xuxin Cheng, Xue Bin Peng, Pieter Abbeel, Sergey Levine, Glen Berseth, and Koushil Sreenath. Reinforcement learning for robust parameterized locomotion control of bipedal robots. In *2021 IEEE International Conference on Robotics and Automation (ICRA)*, pages 2811–2817. IEEE, 2021.
- Yang Zhang, Bo Tang, Qingyu Yang, Dou An, Hongyin Tang, Chenyang Xi, Xueying Li, and Feiyu Xiong. Bcorle (λ): An offline reinforcement learning and evaluation framework for coupons allocation in e-commerce market. *Advances in Neural Information Processing Systems*, 34, 2021.
- Yi Ma, Xiaotian Hao, Jianye Hao, Jiawen Lu, Xing Liu, Tong Xialiang, Mingxuan Yuan, Zhigang Li, Jie Tang, and Zhaopeng Meng. A hierarchical reinforcement learning based optimization framework for large-scale dynamic pickup and delivery problems. *Advances in Neural Information Processing Systems*, 34, 2021.
- Javier Garcia and Fernando Fernández. A comprehensive survey on safe reinforcement learning. *Journal of Machine Learning Research*, 16(1):1437–1480, 2015.
- Baiming Chen, Zuxin Liu, Jiacheng Zhu, Mengdi Xu, Wenhao Ding, Liang Li, and Ding Zhao. Context-aware safe reinforcement learning for non-stationary environments. In *2021 IEEE International Conference on Robotics and Automation (ICRA)*, pages 10689–10695. IEEE, 2021.
- Garrett Thomas, Yuping Luo, and Tengyu Ma. Safe reinforcement learning by imagining the near future. In *Thirty-Fifth Conference on Neural Information Processing Systems*, 2021.
- Krishnakant V. Saboo, Anirudh Choudhary, Yurui Cao, Gregory Worrell, David T Jones, and Ravi Iyer. Reinforcement learning based disease progression model for alzheimer’s disease. In A. Beygelzimer, Y. Dauphin, P. Liang, and J. Wortman Vaughan, editors, *Advances in Neural Information Processing Systems*, 2021. URL <https://openreview.net/forum?id=R4NeFnapYQZ>.
- Brijen Thananjeyan, Ashwin Balakrishna, Suraj Nair, Michael Luo, Krishnan Srinivasan, Minh Hwang, Joseph E Gonzalez, Julian Ibarz, Chelsea Finn, and Ken Goldberg. Recovery rl: Safe reinforcement learning with learned recovery zones. *IEEE Robotics and Automation Letters*, 6(3): 4915–4922, 2021.
- Yinlam Chow, Ofir Nachum, Edgar Duenez-Guzman, and Mohammad Ghavamzadeh. A lyapunov-based approach to safe reinforcement learning. *arXiv preprint arXiv:1805.07708*, 2018.
- Björn Lütjens, Michael Everett, and Jonathan P How. Safe reinforcement learning with model uncertainty estimates. In *2019 International Conference on Robotics and Automation (ICRA)*, pages 8662–8668. IEEE, 2019.

- Richard Cheng, Gábor Orosz, Richard M Murray, and Joel W Burdick. End-to-end safe reinforcement learning through barrier functions for safety-critical continuous control tasks. In *Proceedings of the AAAI Conference on Artificial Intelligence*, volume 33, pages 3387–3395, 2019.
- Daniel Brown, Russell Coleman, Ravi Srinivasan, and Scott Niekum. Safe imitation learning via fast bayesian reward inference from preferences. In *International Conference on Machine Learning*, pages 1165–1177. PMLR, 2020.
- Santiago Paternain, Miguel Calvo-Fullana, Luiz FO Chamon, and Alejandro Ribeiro. Safe policies for reinforcement learning via primal-dual methods. *IEEE Transactions on Automatic Control*, 2022.
- Mohammed Alshiekh, Roderick Bloem, Rüdiger Ehlers, Bettina Könighofer, Scott Niekum, and Ufuk Topcu. Safe reinforcement learning via shielding. In *Thirty-Second AAAI Conference on Artificial Intelligence*, 2018.
- Alexander I Cowen-Rivers, Daniel Palenicek, Vincent Moens, Mohammed Amin Abdullah, Aivar Sootla, Jun Wang, and Haitham Bou-Ammar. Samba: Safe model-based & active reinforcement learning. *Machine Learning*, pages 1–31, 2022.
- Jesse Zhang, Brian Cheung, Chelsea Finn, Sergey Levine, and Dinesh Jayaraman. Cautious adaptation for reinforcement learning in safety-critical settings. In *International Conference on Machine Learning*, pages 11055–11065. PMLR, 2020.
- Romain Laroche, Paul Trichelair, and Remi Tachet Des Combes. Safe policy improvement with baseline bootstrapping. In *International Conference on Machine Learning*, pages 3652–3661. PMLR, 2019.
- harsh satija, Philip S. Thomas, Joelle Pineau, and Romain Laroche. Multi-objective SPIBB: Seldonian offline policy improvement with safety constraints in finite MDPs. In A. Beygelzimer, Y. Dauphin, P. Liang, and J. Wortman Vaughan, editors, *Advances in Neural Information Processing Systems*, 2021. URL <https://openreview.net/forum?id=XzH3QMBKIJ>.
- Matteo Turchetta, Andrey Kolobov, Shital Shah, Andreas Krause, and Alekh Agarwal. Safe reinforcement learning via curriculum induction. *arXiv preprint arXiv:2006.12136*, 2020.
- Janarthanan Rajendran, Aravind Srinivas, Mitesh M Khapra, P Prasanna, and Balaraman Ravindran. Attend, adapt and transfer: Attentive deep architecture for adaptive transfer from multiple sources in the same domain. *arXiv preprint arXiv:1510.02879*, 2015.
- Mohammadamin Barekatin, Ryo Yonetani, and Masashi Hamaya. Multipolar: Multi-source policy aggregation for transfer reinforcement learning between diverse environmental dynamics. *arXiv preprint arXiv:1909.13111*, 2019.
- Nolan C Wagener, Byron Boots, and Ching-An Cheng. Safe reinforcement learning using advantage-based intervention. In *International Conference on Machine Learning*, pages 10630–10640. PMLR, 2021.
- Yonathan Efroni, Shie Mannor, and Matteo Pirota. Exploration-exploitation in constrained mdp. *CoRR*, abs/2003.02189, 2020. URL <https://arxiv.org/abs/2003.02189>.
- Homanga Bharadhwaj, Aviral Kumar, Nicholas Rhinehart, Sergey Levine, Florian Shkurti, and Animesh Garg. Conservative safety critics for exploration. *arXiv preprint arXiv:2010.14497*, 2020.
- Vincent François-Lavet, Peter Henderson, Riashat Islam, Marc G Bellemare, and Joelle Pineau. An introduction to deep reinforcement learning. *arXiv preprint arXiv:1811.12560*, 2018.
- John Schulman, Filip Wolski, Prafulla Dhariwal, Alec Radford, and Oleg Klimov. Proximal policy optimization algorithms. *arXiv preprint arXiv:1707.06347*, 2017.
- Joshua Achiam, David Held, Aviv Tamar, and Pieter Abbeel. Constrained policy optimization. In *International conference on machine learning*, pages 22–31. PMLR, 2017.

- Jun Zeng, Bike Zhang, and Koushil Sreenath. Safety-critical model predictive control with discrete-time control barrier function. In *2021 American Control Conference (ACC)*, pages 3882–3889. IEEE, 2021.
- Yuping Luo and Tengyu Ma. Learning barrier certificates: Towards safe reinforcement learning with zero training-time violations. In *Thirty-Fifth Conference on Neural Information Processing Systems*, 2021.
- Peter Geibel and Fritz Wysotzki. Risk-sensitive reinforcement learning applied to control under constraints. *Journal of Artificial Intelligence Research*, 24:81–108, 2005.
- Chen Tessler, Daniel J Mankowitz, and Shie Mannor. Reward constrained policy optimization. *arXiv preprint arXiv:1805.11074*, 2018.
- Gal Dalal, Krishnamurthy Dvijotham, Matej Vecerik, Todd Hester, Cosmin Paduraru, and Yuval Tassa. Safe exploration in continuous action spaces. *arXiv preprint arXiv:1801.08757*, 2018.
- Akifumi Wachi, Yunyue Wei, and Yanan Sui. Safe policy optimization with local generalized linear function approximations. *Advances in Neural Information Processing Systems*, 34, 2021.
- Jinhua Song, Yang Gao, Hao Wang, and Bo An. Measuring the distance between finite markov decision processes. In *Proceedings of the 2016 international conference on autonomous agents & multiagent systems*, pages 468–476, 2016.
- Romain Laroché and Merwan Barlier. Transfer reinforcement learning with shared dynamics. In *Thirty-First AAAI Conference on Artificial Intelligence*, 2017.
- Fernando Fernández and Manuela Veloso. Probabilistic policy reuse in a reinforcement learning agent. In *Proceedings of the fifth international joint conference on Autonomous agents and multiagent systems*, pages 720–727, 2006.

A Implementation details

A.1 Network architectures

We implement baselines and AASC by using PPO (Schulman et al., 2017) as the base RL model. The **MLP** is a special case of AASC without source policies, which means training from scratch. The MLP of the Circle environment consists of 2 hidden layers, 64 neurons per hidden layer, tanh activation function, with batch size 4000 and discount factor γ 0.99. The threshold σ is 0.01 and penalty value b is -2 and cost constant α is 0.5. The advantage threshold $\eta = 0.08$. Both network parameters are updated using Adam with a learning rate of 10^{-3} . All target networks are updated with a learning rate of 10^{-3} . For the Half-cheetah environment, the network design is the same as the Circle environment and the penalty value b is -0.01 and the cost constant α is 0.05 and $\eta = 0.2$. The same network architecture is also used as a base model in others baselines unless specifically stated.

In **AASC**, the auxiliary network has identical architecture to that of the MLP. Therefore, the only difference between MLP and AASC was the adaptive aggregation part, which makes it possible to evaluate the contribution of transfer learning based on an adaptive aggregation of source policies. The attention network in AASC also has the same architecture as MLP, with the difference in the output layer with softmax function.

For a fair comparison, we also implement the **MULTIPOLAR** with the safeguard evaluation module to illustrate the advantages of using the adaptive aggregation of sources policy. The **MULTIPOLAR** selects source policies through an adjustable matrix. Since **MULTIPOLAR** does not utilize the effects of the input states to adjust the differentiable matrix directly, its ability to adjust the weighted parameters according to the change in the environment is weaker than AASC.

In **Recovery RL**, the unsafe set is defined as $\mathcal{T}_{unsafe}^\pi = \{(s, a) \in S_{safe} \times A : Q(s, a_{task}) \geq \eta\}$, where $\mathcal{T}_{safe}^\pi = S \times A \setminus \mathcal{T}_{unsafe}^\pi$. The value of η is same as in AASC. Plus, the Recovery RL trains the agent with a set of transitions $D_{offline}$ that contain constraint violations for pretraining. Since we don't have the prior knowledge of the target environment, we utilize this pretrained dataset and fine-tune the network in the target task.

In **CARL**, we employ model-based RL to train a probabilistic model to capture uncertainty about transition dynamics and catastrophic states across varied source environments. Then fine-tune on a new task. The parameters are chosen with little modification to the original training parameters of the similar environments in Zhang et al. [2020].

In **CPO**, we guarantee safety in terms of constraint satisfaction that holds in expectation and extends trust-region policy optimization (TRPO) to handle the CMDP constraints, the parameters are the same as in Achiam et al. [2017].

All experiments were run on an NVIDIA GeForce GTX 1070. The given hyperparameters were found by hand-tuning until the good performance was found on all algorithms.

A.2 Environment parameters

The state in Circle environment can be represented as $s = (x, y, \dot{x}, \dot{y})$, where (x, y) is the x-y position and (\dot{x}, \dot{y}) is the corresponding velocity. The action $a = (a_x, a_y)$ is the force applied to the robot (each component has maximum magnitude a_{max}). In our experiments, we set the parameters of target environment to $m = 1, v_{max} = 2, a_{max} = 1, x_{max} = 2.5$, and $y_{max} = 15$. In Half-cheetah environment, we set $h_{min} = 0.4$ and $h_{max} = 1$.

In all experiments, when computing \bar{Q} , we use the cost function which indicates the distance to the unsafe set to make our intervention mechanism reasonable and hence the training process safer. $\hat{c}(s, a)$ is a function of the distance of the state s to the boundary of the unsafe set, denoted by $\text{dist}(s, S_{unsafe})$. For the circle environment, S_{unsafe} denotes the unsafe regions which are outside the vertical lines. The distance function is $\text{dist}(s, S_{unsafe}) = \max\{0, \min\{x_{max} - x, x_{max} + x, y_{max} - y, y_{max} + y\}\}$. For the half-cheetah environment, the distance function $\text{dist}(s, S_{unsafe}) = \max\{0, \min\{h - h_{min}, h_{max} - h\}\}$. For some constant $\alpha \geq 0$, the cost function is defined as a hinge function of the distance as:

$$\hat{c}(s, a) = \begin{cases} \mathbb{1}\{\text{dist}(s, S_{unsafe}) = 0\}, & \alpha = 0 \\ \max\{0, 1 - \frac{1}{\alpha} \text{dist}(s, S_{unsafe})\}, & (\text{otherwise}). \end{cases} \quad (8)$$

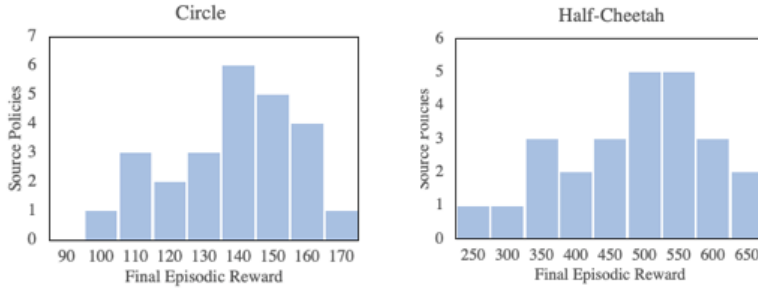


Figure 5: Histogram of final episodic rewards obtained by source policies in their original environment instances.

We note that \hat{c} is an upper bound for c if $\alpha > 0$ and $\hat{c} = c$ if $\alpha = 0$. This cost function is continuous so that the effects of approximation bias are smaller than that resulting from a binary cost 0, 1. The backup policy μ applies a decelerating force (with component-wise magnitude up to a_{max}) until the agent has zero velocity.

A.3 Source policies

For each of the environments, we first created 25 environment instances by randomly sampling the dynamics and kinematics parameters from a specific range. For example, these parameters in the Circle environment were the agent’s mass m , constraint width x_{max} and length y_{max} , max velocity v_{max} defined in the environment and height constraints h_{max} and h_{min} in Halfcheetah. Details of sampling ranges for parameters of all environments are presented in table 1 and 2. Note that we defined the sampling ranges for each environment such that the resulting environment instances are significantly different in dynamics, as shown in figure 1. Figure 5 shows the histograms of final episodic rewards (average rewards of the last 100 training episodes) for the source policy candidates obtained in their original environment instances. As shown in figure 1, the source policies were diverse in terms of performance. Then, for each environment instance, we trained MLP policies as the source policy candidates, from which we sample $I = 4$ of them to train AASC as well as CARL and MULTIPOLAR. Specifically, for each environment instance, we trained three sets of policies each with distinct source policy sets selected randomly from the candidate pool. Plus, the learning procedure explained above was done three times with fixed different random seeds to reduce variance in results due to stochasticity. What’s more, although we used trained MLPs as source policies for reducing experiment times, any type of policy including hand-engineered ones could be used for AASC in principle.

Table 1: Sampling ranges for Circle environment parameters

Factors	Value range
m	[0.5, 1.5]
x_{max}	[0.5, 3.5]
y_{max}	[5, 25]
v_{max}	[1, 3]

Table 2: Sampling ranges for Half-cheetah environment parameters

Factors	Value range
m	[10, 18]
h_{max}	[0.8, 1.2]
h_{min}	[0.2, 0.6]

B Ablation Study

Effect of source policy performances.

In this setup, we investigate the effect of source policy performances on AASC sample efficiency. We select two separate pools of source policies, where one contained only high-performing and the other only low-performing ones. For example, in the Circle environment, the high-performing ones are those with a final episodic reward higher than 150, and the low-performing ones are those under 120. Table 3 summarizes the results of sampling source policies from these pools (4 high, 2 high & 2 low, and 4 low performances) and compares them to the original AASC after 250k and 500k training steps. As shown in this table, AASC can achieve the best performance when all the source policies were sampled from the high-performance pool. However, we emphasize that such high-quality policies are not always available in practice, due to the variability of how they are learned or hand-crafted in their environment instance. Interestingly, by comparing the reported results in table 3 MLP and AASC with 4 low performance, we can observe that even in the worst-case scenario of having only low performing source policies, the sample efficiency of AASC is on par with that of learning from scratch. This suggests that AASC avoids the worse source policy transfer, which occurs when transfer degrades the learning efficiency instead of helping it. Further, AASC successfully learns to suppress the useless low-performing sources to maximize the expected return in a target task, indicating the mechanism of source policy rejection.

Table 3: Results with different source policy sampling in Circle environment

Methods	250k	500k
MLP	86 (80, 94)	125 (117, 138)
AASC (random)	135 (131, 147)	145 (135, 157)
AASC (4 high performance)	156 (152, 160)	158 (152, 163)
AASC (2 high & 2 low performance)	132 (121, 137)	142 (138, 154)
AASC (4 low performance)	85 (84, 98)	126 (119, 140)

Effect of number of source policies.

Besides, we show how the number of source policies contributes to AASC’s sample efficiency in Table 4. Specifically, we trained AASC policies up to $K = 10$ to study how the mean of average episodic rewards changes. The monotonic performance improvement over K for $K \leq 10$ is achieved at the cost of increased inference time. The AASC with $K = 4$ can achieve a competitive performance compared with $K = 10$ considering the computation complexity and the availability of source policies. In practice, we suggest balancing this speed-performance trade-off by using as many source policies as possible before reaching the inference time limit required by the application.

Table 4: Results with different number of source policies in Circle environment

Methods	250k	500k
MLP	86 (80, 94)	125 (117, 138)
AASC ($K = 1$)	127 (125, 135)	138 (136, 142)
AASC ($K = 4$)	135 (131, 147)	145 (135, 157)
AASC ($K = 10$)	137 (133, 150)	150 (140, 160)